

The onset of magnetism peaked around $x = 1/4$ in optimally electron-doped $\text{LnFe}_{1-x}\text{Ru}_x\text{AsO}_{1-y}\text{F}_y$ (Ln = La, Nd or Sm) superconductors

S. Sanna,¹ P. Carretta,¹ R. De Renzi,² G. Prando,^{1,3} P. Bonfá,²

M. Mazzani,² G. Lamura,⁴ T. Shiroka,^{5,6} Y. Kobayashi,⁷ M. Sato⁷

¹ *Department of Physics, University of Pavia-CNISM, I-27100 Pavia, Italy*

² *Department of Physics and Earth Sciences, University of Parma-CNISM, I-43121 Parma, Italy*

³ *Leibniz-Institut für Festkörper- und Werkstoffforschung (IFW) Dresden, D-01171 Dresden, Germany*

⁴ *CNR-SPIN and Università di Genova, via Dodecaneso 33, I-16146 Genova, Italy*

⁵ *Laboratorium für Festkörperphysik, ETH-Hönggerberg, CH-8093 Zürich, Switzerland*

⁶ *Paul Scherrer Institut, CH-5232 Villigen PSI, Switzerland and*

⁷ *Department of Physics, Division of Material Science, Nagoya University, Furo-cho, Chikusa-ku, Nagoya 464-8602, Japan*

(Dated: January 24, 2020)

The appearance of static magnetism, nanoscopically coexisting with superconductivity, is shown to be a general feature of optimally electron-doped $\text{LnFe}_{1-x}\text{Ru}_x\text{AsO}_{1-y}\text{F}_y$ superconductor (Ln - lanthanide ion) upon isovalent substitution of Fe by Ru. The magnetic ordering temperature T_N and the magnitude of the internal field display a dome-like dependence on x , peaked around $x = 1/4$, with higher T_N values for those materials characterized by a larger z cell coordinate of As. Remarkably, the latter are also those with the highest superconducting transition temperature (T_c) for $x = 0$. The reduction of $T_c(x)$ is found to be significant in the x region of the phase diagram where the static magnetism develops. Upon increasing the Ru content superconductivity eventually disappears, but only at $x \simeq 0.6$.

PACS numbers: 74.70.Xa, 74.62.Dh, 76.75.+i, 74.25.Ha

I. INTRODUCTION

The proximity of the magnetic and superconducting ground states is a common aspect of several strongly correlated electron systems, ranging from the heavy fermions, to the organic materials and to the high-temperature superconductors.¹ Also in the iron-based materials² superconductivity emerges close to the disruption of a static magnetic order.^{3–7} Many studies on the transition from the magnetic to the superconducting ground-state have been carried out in these materials, either by varying the electron doping or by applying a high hydrostatic pressure.^{4–15} In several compounds of the $\text{LnFeAsO}_{1-y}\text{F}_y$ family (referred to as Ln1111), with Ln a lanthanide ion, evidence for a nanoscopic coexistence of the superconducting and magnetic states has emerged,^{5–8} similarly to other Fe-based compounds.^{11–15} The stability of these two ground states can be investigated by perturbing the system with, for example, a chemical substitution. In this respect the effect of the Ru-for-Fe isovalent diamagnetic substitution is particularly interesting. In the $y = 0$ Ln1111 case this substitution leads to a progressive dilution of the magnetic lattice^{16–18} and, eventually, to the disappearance of the magnetic order for $x \rightarrow x_c \simeq 0.6$, which is considered to be the percolation threshold for the $J_1 - J_2$ localized spin system.¹⁸

In the optimally F-doped Ln1111 superconductor, Ru substitution leads to the progressive reduction of the superconducting transition temperature T_c [19,20] and to its complete suppression at a Ru concentration close to x_c .²¹ In optimally F-doped Sm1111, besides diluting

the Fe magnetic lattice, Ru has another remarkable effect: it induces a frozen short-range (SR) magnetic order which coexists nanoscopically with superconductivity albeit with reduced T_c values.²¹

In this work we show that the appearance of static SR magnetic order, nanoscopically coexisting with superconductivity, is a common feature of Ru-doped $\text{LnFe}_{1-x}\text{Ru}_x\text{AsO}_{1-y}\text{F}_y$ (hereafter Ln11Ru11) with: Ln = Sm, Nd or La, and with a F content close to optimal doping. The magnetic dome is peaked around the Ru concentration $x = 1/4$ and its extension increases upon decreasing the size of the Ln ion (since the latter is correlated with the cell coordinate of As, z_{As} , hereafter different Ln shall also be identified by their z values). On the other hand, the superconducting transition temperature T_c drops at low Ru content, more abruptly for Ln = Sm, Nd and only marginally for La, at the same Ru content that marks the appearance of the static SR magnetic order at T_N .

II. EXPERIMENTAL DETAILS

To investigate the influence of Ru substitution on the magnetic and superconducting properties of $\text{LnFe}_{1-x}\text{Ru}_x\text{AsO}_{1-y}\text{F}_y$, zero- (ZF) and longitudinal-field (LF) muon-spin spectroscopy (μSR) experiments were performed in powder samples with Ln = La, Nd, prepared as reported in Ref. 20. The μSR experiments have been performed at the Paul Scherrer Institute on the GPS and DOLLY spectrometers. ZF experiments can detect the presence of spontaneous magnetic ordering,

also in case of short-range order.^{7,22} LF experiments, instead, reveal the static or dynamic nature of the magnetic state.²² All the samples were optimally electron-doped with a nominal F content $y = 0.15$ and 0.11 for $\text{Ln}=\text{Sm}$ and for $\text{Ln}=\text{La}$, Nd respectively. Here we compare the $\text{Ln}=\text{La}$ and Nd cases with our published Sm data.²¹ The three families display $T_c = 28$ K, 47 K, 52 K for $x = 0$, respectively.

III. RESULTS

A. Detection of static magnetic order

For each one of the Ln families under investigation, a few representative time-dependent ZF- μSR asymmetries curves are shown in the left panels of Fig. 1, together with the best fit to the sum of a longitudinal and a transverse component as:

$$\frac{A_{\text{ZF}}(t)}{a_{\text{ZF}}} = \sum_{i=1,2} \left(w_{L_i} e^{-\lambda_i t} + w_{T_i} e^{-\sigma_i^2 t^2 / 2} \right) \quad (1)$$

where $\sum_i (w_{L_i} + w_{T_i}) = 1$, a_{ZF} is the total muon signal amplitude, calibrated at high temperature in the paramagnetic phase, w_L and w_T are the weights of the transverse and longitudinal terms, respectively, and λ and σ are the corresponding decay rates. The transverse term is an overdamped precession, due to a static mean internal field \bar{B} comparable to the square-root of the second moment $\Delta B = \sigma/\gamma$ (with $\gamma/2\pi = 135.5$ MHz/T the muon gyromagnetic ratio). Indeed, LF measurements show that for all the Ln families an external field of the order of ΔB is sufficient to quench the transverse relaxation, revealing the static character of the magnetic state. The subscript $i = 1, 2$, when applicable, accounts for the two known muon stopping sites in $\text{Ln}1111$ compounds,^{30–32} one from within the FeAs layers and the other close to O^{2-} ions. The two longitudinal components w_{L_i} are well resolved only for $\text{Ln}=\text{Sm}$, as for the non magnetic $\text{Sm}1111$ case.³³

The magnitude of the internal magnetic fields B_i at the muon site ($\simeq \Delta B_i$ shown in Fig. 1e) is the sum of the fields generated by the static moments surrounding the muon site, which depend on the distribution of Fe and Ru atoms at the neighboring sites. Notice that the fast decay of the transverse component starts well above the Ln (Sm or Nd) ordering temperature, hence it must be related to the static Fe moments. At $T \rightarrow 0$ K the mean value of the internal fields for $\text{Ln} = \text{Sm}$ is about 40 mT, while it decreases to ~ 20 mT for $\text{Ln} = \text{La}$ and Nd . These are the typical values measured in F-doped $\text{Ln}1111$ compounds close to the crossover between the magnetic and superconducting phases, of $\text{Ln}=\text{Sm}$ and Ce [5,34] and La [10,31].

For polycrystals, the volume fraction in which muons experience a net internal field can be calculated as V_{mag}

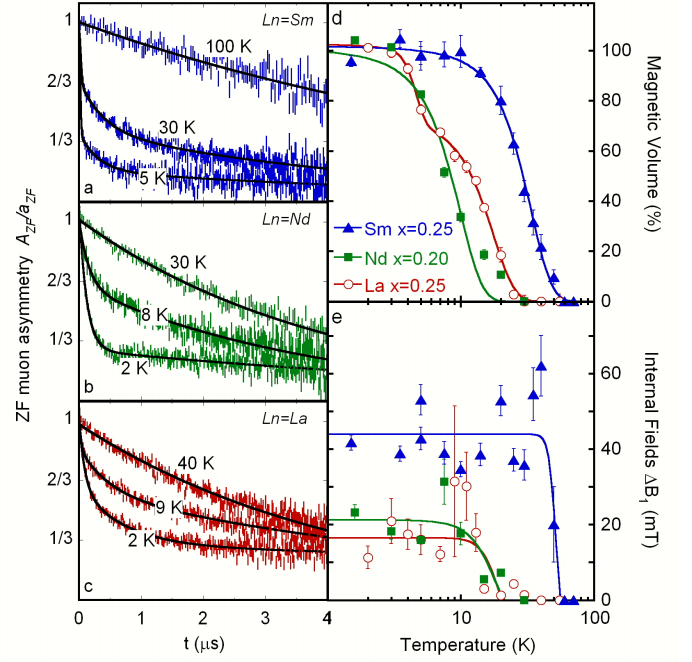


FIG. 1. (Color online) ZF- μSR in optimally F-doped $\text{LnFe}_{1-x}\text{Ru}_x\text{AsO}_{1-y}\text{F}_y$ at $x \sim 0.25$, with a nominal F content $y = 0.15$ and 0.11 for $\text{Ln}=\text{Sm}$ and for $\text{Ln}=\text{La}$, Nd respectively. Time dependence of the normalized muon asymmetry for $\text{Ln} = \text{Sm}$ (a), Nd (b) and La (c). The lines represent the best fits according to Eq. (1). Panels (d) and (e) show the volume fraction V_{mag} , where muons detect an internal magnetic field, and the root mean-square value of the internal field at the muon site ΔB_1 , respectively, as a function of temperature (see text for details).

$= 3 \sum_i w_{T_i} / 2 = 3(1 - \sum_i w_{L_i}) / 2$.^{5,34} The ordering temperatures T_N plotted in Fig. 2b are determined from the condition $V_{\text{mag}}(T_N) = 0.5$. Figure 1d shows that $V_{\text{mag}} = 1$ at low temperature for all the three $\text{Ln}11\text{Ru}11$ compounds. It is important to notice that the estimated dipolar field distribution of width ΔB_1 implies a distribution of distances $0.1 \lesssim r \lesssim 2$ nm between the muon and the closest frozen Fe moment.⁵

B. The 3D phase diagram

Our main result is displayed in Fig. 2. The top panel shows the behavior of the superconducting transition temperature T_c for the three $\text{Ln}11\text{Ru}11$ families, as determined by DC superconducting quantum interference device (SQUID) magnetization measurements (see Ref. 20 and 21). The bottom panel reports the corresponding magnetic ordering temperatures, from μSR . A remarkable feature is the rather pronounced suppression of T_c for $\text{Ln} = \text{Sm}$ and Nd at $x \simeq 0.10$ and 0.20 , respectively. As already shown²¹ for $\text{Ln} = \text{Sm}$ this concentration co-

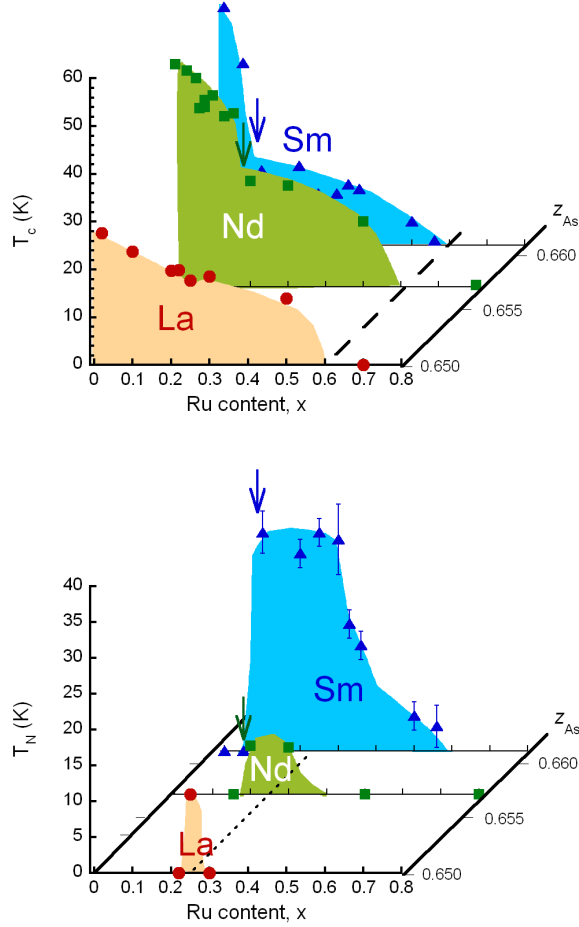


FIG. 2. (Color online) Transition temperatures in optimally F-doped $\text{LnFe}_{1-x}\text{Ru}_x\text{AsO}_{1-y}\text{F}_y$ (nominal $y = 0.15$ and 0.11 for $\text{Ln}=\text{Sm}$ and for $\text{Ln}=\text{La}$, Nd respectively), as a function of the Ru content x and the z_{As} cell coordinate. Top, superconducting temperatures T_c from dc magnetization measurements reported in Ref. 20 and 21; bottom, magnetic ordering temperatures T_N as from μSR measurements. The vertical arrows indicate the $x = 0.1$ and 0.2 Ru-substitution levels in $\text{Ln} = \text{Sm}$ and Nd , respectively. The dashed and dotted lines mark the magnetic percolation threshold $x_c \simeq 0.6$ and the T_N peak value at $x = 1/4$, respectively.

incides with the onset of static SR magnetic order (see Fig. 2 bottom panel). A very similar behavior is observed also in case of $\text{Ln}=\text{Nd}$ at $x \simeq 0.2$. T_c vanishes for *all* the families around $x \rightarrow 0.6$, which corresponds to the magnetic percolation threshold x_c for the magnetic lattice in the undoped La111 .¹⁸

In addition it is interesting to note that, despite the low density of $\text{Ln}=\text{Nd}$ points, both La and Sm data give evidence that the maximum of T_N is peaked around $x = 0.25$. In the bottom panel of Fig. 2 this indication is very sharp for $\text{Ln}=\text{La}$. For $\text{Ln}=\text{Sm}$, although asymmetric, T_N has again a maximum around $x = 0.25$.

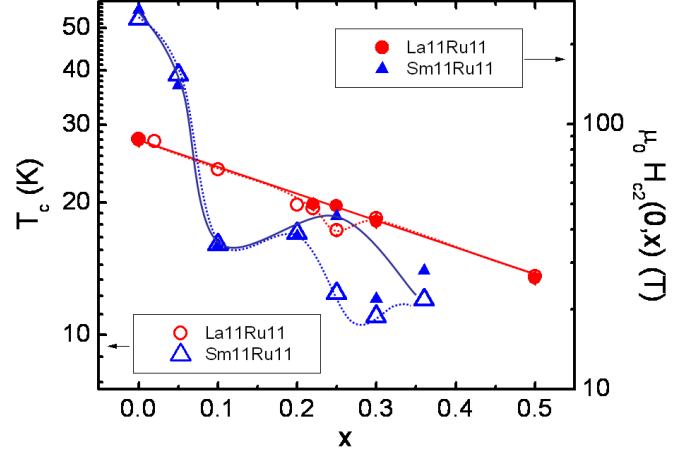


FIG. 3. (Color online) Superconducting T_c (open symbols, left scale) and $H_{c2}(T \rightarrow 0)$ (closed symbols, right scale), vs. Ru content x in $\text{SmFe}_{1-x}\text{Ru}_x\text{AsO}_{0.85}\text{F}_{0.15}$ (triangles) and in $\text{LaFe}_{1-x}\text{Ru}_x\text{AsO}_{0.89}\text{F}_{0.11}$ (circles). The lines are guides to the eye.

C. Nanoscopic coexistence of magnetism and superconductivity

We found that V_{mag} is close to unity below T_N for all the magnetic samples with nonzero T_N . This implies that in the absence of an applied field all ZF implanted muons detect the presence of an ordered magnetic moment, i.e. internal fields develop throughout the whole sample (although some muons detect these fields from just outside a magnetic region, not farther than a few nm). Since dc magnetometry measurements detect a sizeable superconducting fraction,^{20,21} following the same arguments used in Refs. 21 and 34, it is conceivable that in all these families magnetic and superconducting regions form an interspersed texture, owing to the nanoscopic electronic inhomogeneities induced by the Ru distribution.

However superconductivity may survive in such finely dispersed regions only as long as its coherence length ξ is comparable to the average separation r (few nm) among magnetic domains. In order to roughly estimate the coherence length ξ_x as a function of Ru content x , the upper critical field $H_{c2}(T, x) \propto \xi_x^{-2}$ was derived²³ for $\text{Ln} = \text{La}$. The data for $\text{Ln} = \text{Sm}$ are taken from Ref. 19. The value of H_{c2} for $T \rightarrow 0$ was estimated from the Werthamer-Helfand-Hohenberg relation²⁴

$$H_{c2} \simeq 0.7 \times T_c(H=0) |dH_{c2}/dT|_{T_c(x, H=0)} . \quad (2)$$

Although this expression tends to overestimate²⁵ $H_{c2}(0, x)$, it can still provide the relative variation of the upper critical field with Ru substitution. The results are shown in Fig. 3 for $\text{Ln} = \text{La}$ (solid circles) and Sm (solid triangles). One can then derive ξ_x and find that $\xi_{0.25}/\xi_0$ is 1.3 and 2.4 for La and Sm , respectively. Hence, from

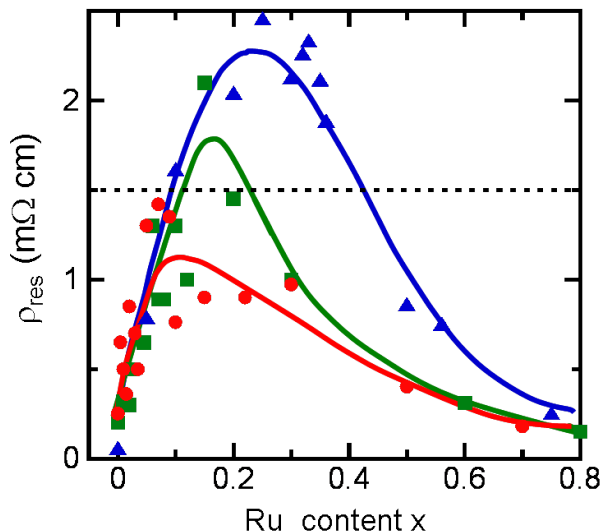


FIG. 4. (Color online) Residual resistivity as a function of Ru content for $\text{LnFe}_{1-x}\text{Ru}_x\text{AsO}_{0.89}\text{F}_{0.11}$ with $\text{Ln}=\text{La}$ (circle), Nd (square) and Sm (triangle) families, using data reported in Ref.[20] and [19].

the absolute values of ξ_0 reported in Ref. 23 one estimates an absolute value $\xi_{0.25} \approx 3$ nm for both Ln ions, namely the same order of magnitude of the mean distance r among magnetic domains. Thus, the observation of bulk superconductivity does not conflict with muons detecting $V_{mag} = 1$ (Fig. 1d).

The nanoscopic coexistence of the two phases in Ln11Ru11 is reminiscent of that observed at the crossover between magnetic and superconducting order in F-doped Sm1111 ^{5,6} and Ce1111 ³⁴, but notably not in La1111 . In the latter the two order parameters are mutually exclusive at ambient pressure⁴ and are observed to coexist in mesoscopically separated regions under both external¹⁰ and chemical³⁵ pressures. Here, the detection of nanoscopic coexistence not only in Sm11Ru11 and Nd11Ru11 , but also in La11Ru11 , suggests that the substitution of Fe with the isovalent non magnetic Ru induces a static SR magnetic order.

IV. DISCUSSION

Our results show that the static SR magnetic order induced by the isovalent and nonmagnetic Ru substitution around $x = 1/4$ is a common aspect of $\text{LnFe}_{1-x}\text{Ru}_x\text{AsO}_{1-y}\text{F}_y$ optimally F-doped superconductors.

A possible mechanism which explains the observed suppression of T_c and the appearance of a static SR magnetic order is the electron localization, arising from Ru impurity scattering. This localizing effect is well known to suppress the superconducting transition temperature²⁶. In addition, due to the loss of the kinetic energy of the

electrons, which becomes significant as the temperature decreases, electron localization may induce local magnetic moments on the Fe ions which eventually freeze below T_N .

The above idea is supported by the x dependence of the residual resistivity, ρ_{res} , which for all $\text{Ln} = \text{La}$, Nd ²⁰ and Sm ¹⁹ compounds displays a behavior analogous to the one of $T_N(x)$, as shown in Fig. 4. This dome-like trend indicates a competition between the electron localization and the increase in kinetic energy caused by the more extended Ru d orbitals. Interestingly, at least for Sm and Nd, the maximum of the residual resistivity is close to $x = 1/4$ where $T_N(x)$ is peaked. Moreover, a direct comparison with Fig. 2b indicates that the magnetic state can develop only for those samples with $\rho_{res} \gtrsim \rho_c = 1.5 \text{ m}\Omega\text{cm}$ (emphasized by the dotted line), which is quite reasonable as a crossover value for Anderson localization.²⁷

In a slightly different scenario, one can consider that the perturbation generated by Ru impurity yields a staggered polarization of the magnetic moments present on the surrounding Fe sites. This hypothesis is based on the experimental evidence for the existence of a sizeable, rapidly fluctuating magnetic moment at the Fe site in different optimally doped Fe-based superconductors.^{36,37} Then, one could expect that when these moments freeze, a static SR order appears, characterized by antiferromagnetic correlations analogous to those observed in the underdoped $\text{Ln}=\text{Sm}$, Ce [5,34] and $\text{Ln}=\text{La}$ [10] compounds close to the crossover between magnetic and superconducting phases. In fact, the μSR spectra shown in Fig. 1 at $x \simeq 1/4$ are very similar to those measured at that crossover. Specifically, no oscillations are observed in the time spectra and the depolarization rates of the transverse fractions measured here for $T \rightarrow 0$, when $\text{Ln}=\text{Sm}$ or La , are similar to those of the F-doped Ln1111 compounds close to the crossover between magnetic and superconducting phases, namely σ_1 is of about $60 \mu\text{s}^{-1}$ [9] and $20 \mu\text{s}^{-1}$ [14], respectively.

We notice that the appearance of static magnetism (around $x = 0.1$, $\text{Ln}=\text{Sm}$ and $x = 0.2$, $\text{Ln}=\text{Nd}$, arrows in the top and bottom panels of Fig. 2) is concomitant with a marked change of the derivative $dT_c(x)/dx$. Figure 3 shows that the critical field $H_{c2}(x)$ generally follows the same trend of $T_c(x)$ for both Sm and La, with the notable exception of the $x \simeq 0.25$ compositions, where T_c is more drastically depressed in both families. The effect is more sizeable when the SR magnetic order is stronger ($\text{Ln}=\text{Sm}$, Fig. 2). The comparison of Sm and La at $x = 0.1$ indicates that the onset of magnetic order in Sm11Ru11 depresses T_c well below the value of the corresponding La11Ru11 , where the static SR magnetic order is absent. This behavior indicates that the *static* magnetism and superconductivity in 1111 do strongly compete. In other words, T_c seems to be reduced by the renormalization of the spectrum of the spin fluctuations, induced by the onset of the static SR order, suggesting that superconductivity is driven by a spin fluctuation mecha-

nism. This observation appears to be in agreement with recent point-contact Andreev-reflection measurements³⁸ performed on the same set of Sm11Ru11 samples, which indicate a progressive decrease of the boson energy when static magnetism appears.

The static magnetic order is more extended and accompanied by larger internal fields ΔB_1 in those compounds where the superconducting T_c for the Ru free $x = 0$ composition is higher. Indeed, both ΔB_1 and T_c increase from La to Sm, together with the z cell coordinate of As,^{39,40} (oblique axis in Fig. 2) that is very little Ru dependent^{19,41}. This trend is in agreement with Landau free energy derivation, based on density functional calculations in the local density approximation, showing that the magnetic ground-state in Ln1111 compounds gets progressively more stable as z increases.²⁸ The same calculations suggest that the z_{As} coordinate may effectively tune the approach to a Quantum Tricritical Point (QTP) where an enhancement of the superconducting pairing may occur.

On the other hand, it should be pointed out that the strong competition between the superconductivity and the static SR magnetic order can be understood even when the pairing mechanism is not related to the spin-fluctuations. Actually, the s_{\pm} symmetry expected in case of spin-fluctuation mechanism can hardly explain the very small initial T_c -suppression rate $|dT_c/dx|_{x \rightarrow 0}$ observed in these systems,⁴²⁻⁴⁴ unless the intra-band impurity scattering is much larger than the inter-band one.⁴⁵⁻⁴⁷ On this point, it is worth mentioning that theories which predict a possible role of the orbital fluctuations⁴⁸⁻⁵⁰ predict an s_{++} symmetry of the order parameter, which can explain the small values of $|dT_c/dx|_{x \rightarrow 0}$ observed here.

V. CONCLUSION

In conclusion, the phase diagram of Ru-doped $\text{LnFeAsO}_{1-y}\text{F}_y$ with optimum value of y was outlined for different Ln ions. It was shown that the appearance of static magnetism induced by the nonmagnetic isovalent Ru substitution around $x = 1/4$ is a common aspect of $\text{LnFe}_{1-x}\text{Ru}_x\text{AsO}_{1-y}\text{F}_y$ optimally F-doped superconductors. The onset of the magnetism is concomitant to a sizeable weakening of the superconducting state in the x region where the residual resistivity shows a peak, namely where the effects of the electron localization are most significant. The stronger the static magnetism induced by Ru substitution, the more significant is the degradation of the superconducting state, which is definitely suppressed only for $x \rightarrow x_c \simeq 0.6$. In addition, it was shown that the magnitude of the transition temperature T_N and the x extension of the magnetic phase appear to progressively vanish as one moves in the $x - z_{As}$ plane towards lower z_{As} values while x is kept at $\sim 1/4$. These results were discussed in the framework of different superconducting pairing mechanisms.

ACKNOWLEDGMENTS

This work was performed at the Swiss Muon Source μS , Paul Scherrer Institut (PSI, Switzerland) and was partially supported by Fondazione Cariplo (research grant no. 2011-0266) and by MIUR-PRIN grant 2008XWLF9-04. T.S. acknowledges support from the Schweizer Nationalfonds (SNF) and the NCCR program MaNEP. G.P. acknowledges support from the Leibniz-Deutscher Akademischer Austauschdienst (DAAD) Post-Doc Fellowship Program. The assistance by Alex Amato and Hubertus Luetkens during the μSR measurements at PSI is gratefully acknowledged.

¹ M. Capone, M. Fabrizio, C. Castellani, E. Tosatti, *Rev. Mod. Phys.* **81** 943 (2009).

² Y. Kamihara, T. Watanabe, M. Hirano, and H. Hosono, *J. Am. Chem. Soc.* **130**, 3296 (2008).

³ J. Zhao, Q. Huang, C. de la Cruz, Shiliang Li, J. W. Lynn, Y. Chen, M. A. Green, G. F. Chen, G. Li, Z. Li, J. L. Luo, N. L. Wang and P. Dai, *Nature Mater.* **7**, 953 (2008).

⁴ H. Luetkens, H.-H. Klauss, M. Kraken, F. J. Litterst, T. Dellmann, R. Klingeler, C. Hess, R. Khasanov, A. Amato, C. Baines, M. Kosmala, O. J. Schumann, M. Braden, J. Hamann-Borrero, N. Leps, A. Kondrat, G. Behr, J. Werner, B. Büchner, *Nature Mater.* **8**, 305 (2009).

⁵ S. Sanna, R. De Renzi, G. Lamura, C. Ferdeghini, A. Palenzona, M. Putti, M. Tropeano, and T. Shiroka, *Phys. Rev. B* **80**, 052503 (2009).

⁶ A. J. Drew, F. L. Pratt, T. Lancaster, S. J. Blundell, P. J. Baker, R. H. Liu, G. Wu, X. H. Chen, I. Watanabe, V. K. Malik, A. Dubroka, K. W. Kim, M. Rössle and C. Bernhard, *Nature Mater.* **8**, 310 (2009).

⁷ T. Shiroka, G. Lamura, S. Sanna, G. Prando, R. De Renzi, M. Tropeano, M. R. Cimberle, A. Martinelli, C. Bernini,

A. Palenzona, R. Fittipaldi, A. Vecchione, P. Carretta, A. S. Siri, C. Ferdeghini, and M. Putti, *Phys. Rev. B* **84**, 195123 (2011).

⁸ H. Maeter, J. E. Hamann-Borrero, Ti. Goltz, J. Spehling, A. Kwadrin, A. Kondrat, L. Veyrat, G. Lang, H.-J. Grafe, C. Hess, G. Behr, B. Büchner, H. Luetkens, C. Baines, A. Amato, N. Leps, R. Klingeler, R. Feyerherm, D. Argyriou, H.-H. Klauss, arXiv:1210.6959

⁹ G. Lang, H.-J. Grafe, D. Paar, F. Hammerath, K. Manthey, G. Behr, J. Werner, and B. Büchner, *Phys. Rev. Lett.* **104**, 097001 (2010)

¹⁰ R. Khasanov, S. Sanna, G. Prando, Z. Shermadini, M. Bendele, A. Amato, P. Carretta, R. De Renzi, J. Karpinski, S. Katrych, H. Luetkens, N. D. Zhigadlo, *Phys. Rev. B* **84**, 100501(R) (2011).

¹¹ M.-H. Julien, H. Mayaffre, M. Horvatić, C. Berthier, X. D. Zhang, W. Wu, G. F. Chen, N. L. Wang and J. L. Luo, *Europhys. Lett.* **87**, 37001 (2009).

¹² E. Wiesenmayer, H. Luetkens, G. Pascua, R. Khasanov, A. Amato, H. Potts, B. Banusch, H.-H. Klauss, and D. Johrendt, *Phys. Rev. Lett.* **107**, 237001 (2011).

- ¹³ Z. Shermadini, H. Luetkens, R. Khasanov, A. Krzton-Maziopa, K. Conder, E. Pomjakushina, H.-H. Klauss, and A. Amato, Phys. Rev. B **85**, 100501(R) (2012).
- ¹⁴ Y. Texier, J. Deisenhofer, V. Tsurkan, A. Loidl, D. S. Inosov, G. Friemel, and J. Bobroff, Phys. Rev. Lett. **108**, 237002 (2012).
- ¹⁵ M. Bendele, A. Ichsanow, Yu. Pashkevich, L. Keller, Th. Strässle, A. Gusev, E. Pomjakushina, K. Conder, R. Khasanov, H. Keller, Phys. Rev. B **85**, 064517 (2012).
- ¹⁶ M. A. McGuire, D. J. Singh, A. S. Sefat, B. C. Sales, D. Mandrus, J. Solid State Chem. **182**, 2326 (2009).
- ¹⁷ Y. Yiu, V. O. Garlea, M. A. McGuire, A. Huq, D. Mandrus, S. E. Nagler, Phys. Rev. B **86**, 054111 (2012).
- ¹⁸ P. Bonfà, P. Carretta, S. Sanna, G. Lamura, G. Prando, A. Martinelli, A. Palenzona, M. Tropeano, M. Putti, R. De Renzi, Phys. Rev. B **85**, 054518 (2012).
- ¹⁹ M. Tropeano, M. R. Cimberle, C. Ferdeghini, G. Lamura, A. Martinelli, A. Palenzona, I. Pallecchi, A. Sala, I. Sheikin, F. Bernardini, M. Monni, S. Massidda, M. Putti, Phys. Rev. B **81**, 184504 (2010).
- ²⁰ E. Satomi, S. C. Lee, Y. Kobayashi, M. Sato, J. Phys. Soc. Jpn. **79** 094702 (2010); S. C. Lee, E. Satomi, Y. Kobayashi, M. Sato, J. Phys. Soc. Jpn. **79** (2010) 023702.
- ²¹ S. Sanna, P. Carretta, P. Bonfà, G. Prando, G. Allodi, R. De Renzi, T. Shiroka, G. Lamura, A. Martinelli, and M. Putti Phys. Rev. Lett. **107**, 227003 (2011).
- ²² A. Yaouanc and P. Dalmas de R  otier, Muon Spin Rotation, Relaxation, and Resonance: Applications to Condensed Matter (Oxford University Press, Oxford, 2011).
- ²³ G. Prando, P. Carretta, R. De Renzi, S. Sanna, A. Palenzona, M. Putti, M. Tropeano, Phys. Rev. B **83**, 174514 (2011); G. Prando, P. Carretta, R. De Renzi, S. Sanna, H.-J. Grafe, S. Wurmehl, B. B  chner, Phys. Rev. B **85**, 144522 (2012).
- ²⁴ N. R. Werthamer, E. Helfand, P. C. Hohenberg, Phys. Rev. **147**, 295 (1966).
- ²⁵ G. Fuchs, S.-L. Drechsler, N. Kozlova, M. Bartkowiak, J. E. Hamann-Borrero, G. Behr, K. Nenkov, H.-H. Klauss, H. Maeter, A. Amato, H. Luetkens, A. Kwadrin, R. Khasanov, J. Freudenberger, A. K  hler, M. Knapfer, E. Arushanov, H. Rosner, B. B  chner, L. Schultz, New J. Phys. **11**, 075007 (2009).
- ²⁶ P. G. de Gennes in *Superconductivity of Metals and Alloys* (Addison-Wesley, New York, 1992).
- ²⁷ A. S. Sefat, J. E. Greedan, G. M. Luke, M. Ni  wczas, J. D. Garrett, H. Dabkowska, A. Dabkowski, Phys. Rev. B **74**, 104419 (2006).
- ²⁸ G. Giovannetti, C. Ortix, M. Marsman, M. Capone, J. van den Brink, J. Lorenzana, Nature Comm. **2**, 398 (2011).
- ²⁹ J. M. Tranquada, B. J. Sternlieb, J. D. Axe, Y. Nakamura, S. Uchida, Nature **375**, 561 (1995).
- ³⁰ H. Maeter, H. Luetkens, Yu. G. Pashkevich, A. Kwadrin, R. Khasanov, A. Amato, A. A. Gusev, K. V. Lamonova, D. A. Chervinskii, R. Klingeler, C. Hess, G. Behr, B. B  chner, and H.-H. Klauss, Phys. Rev. B **80**, 094524 (2009).
- ³¹ G. Prando, P. Bonf  , G. Profeta, R. Khasanov, F. Bernardini, M. Mazzani, E. M. Br  ning, A. Pal, V. P. S. Awana, H.-J. Grafe, B. B  chner, R. De Renzi, P. Carretta, and S. Sanna Phys. Rev. B **87**, 064401 (2013).
- ³² R. De Renzi, P. Bonf  , M. Mazzani, S. Sanna, G. Prando, P. Carretta, R. Khasanov, A. Amato, H. Luetkens, M. Bendele, F. Bernardini, S. Massidda, A. Palenzona, M. Tropeano, M. Vignolo, Supercond. Sci. Technol. **25**, 084009 (2012).
- ³³ R. Khasanov, H. Luetkens, A. Amato, H. H. Klauss, Z. A. Ren, J. Yang, W. Lu, Z. X. Zhao, Phys. Rev. B **78**, 092506 (2008).
- ³⁴ S. Sanna, R. De Renzi, T. Shiroka, G. Lamura, G. Prando, P. Carretta, M. Putti, A. Martinelli, M. R. Cimberle, M. Tropeano, and A. Palenzona, Phys. Rev. B **82**, 060508(R) (2010).
- ³⁵ G. Prando, S. Sanna, G. Lamura, T. Shiroka, M. Tropeano, A. Palenzona, H.-J. Grafe, B. B  chner, P. Carretta, R. De Renzi Phys. Status Solidi B **250**, 599 (2013).
- ³⁶ M. Liu, L. W. Harriger, H. Luo, M. Wang, R. A. Ewings, T. Guidi, H. Park, K. Haule, G. Kotliar, S. M. Hayden, P. Dai, Nature Physics **8**, 376 (2012).
- ³⁷ P. Vilmercati, A. Fedorov, F. Bondino, F. Offi, G. Panaccione, P. Lacovig, L. Simonelli, M. A. McGuire, A. S. M. Sefat, D. Mandrus, B. C. Sales, T. Egami, W. Ku, and N. Mannella, Phys. Rev. B **85**, 220503(R) (2012).
- ³⁸ D. Daghero, M. Tortello, G. A. Ummarino, V. A. Stepanov, F. Bernardini, M. Tropeano, M. Putti, R. S. Gonnelli, Supercond. Sci. Technol. **25**, 084012 (2012).
- ³⁹ A. Iadecola, S. Agrestini, M. Filippi, L. Simonelli, M. Fratini, B. Joseph, D. Mahajan, N. L. Saini Europhys. Lett. **87** 26005 (2009).
- ⁴⁰ D. C. Johnston, Adv. Phys. **59**, 803 (2010).
- ⁴¹ A. Iadecola, B. Joseph, L. Simonelli, L. Maugeri, M. Fratini, A. Martinelli, A. Palenzona, M. Putti, N. L. Saini, Phys. Rev. B **85**, 214530 (2012).
- ⁴² S. Onari and H. Kontani, Phys. Rev. Lett. **103**, 177001 (2009).
- ⁴³ M. Sato, Y. Kobayashi, S. C. Lee, H. Takahashi, E. Satomi, Y. Miura, J. Phys. Soc. Jpn. **79**, 14710 (2010).
- ⁴⁴ M. Sato and Y. Kobayashi, Solid State Commun. **152**, 688 (2012).
- ⁴⁵ R. M. Fernandes, M. G. Vavilov, A. V. Chubukov, Phys. Rev. B **85**, 140512 (2012).
- ⁴⁶ M. G. Vavilov and A. V. Chubukov, Phys. Rev. B **84**, 214521 (2011).
- ⁴⁷ Y. Wang, A. Kreisel, P. J. Hirschfeld, V. Mishra, Phys. Rev. B **87**, 094504 (2013).
- ⁴⁸ H. Kontani and S. Onari, Phys. Rev. Lett. **104**, 157001 (2010).
- ⁴⁹ Y. Yanagi, Y. Yamakawa and Y. Ono, Phys. Rev. B **81**, 054518 (2010).
- ⁵⁰ S. Onari and H. Kontani, Phys. Rev. Lett. **109**, 137001 (2012).